DOI: https://doi.org/10.14311/ISPS.2021.003

Aluminium modification as indicator for current filaments under repetitive short-circuit in 650 V IGBTs

[1]Madhu-Lakshman Mysore, [1]Thomas Basler, [1]Josef Lutz, [2]Roman Baburske, [2]Hans-Joachim Schulze, [2]Franz-Josef Niedernostheide
[1]Chemnitz University of Technology, Chair of Power Electronics, Chemnitz, Germany,
Tel: +49 371/531-36091
[2]Infineon Technologies AG, Neubiberg, Germany

Abstract

In this work, an investigation of the top-side aluminium (Al) metallization modification, under repetitive short-circuit (SC) type I measurements, was carried out for 650 V IGBTs. These measurements were performed far beyond the safe operating area (SOA). The presence of current density filaments at the collector side during SC leads to a local temperature increase that reconstructs the emitter metallization and thus leads to a modification of the top Al surface. Here, the optical microscope was used to observe the change in emitter surface metallization. For 650 V IGBTs, a uniform Al modification pattern was observed irrespective of DC-link voltage and SC pulse width, which is in contrast to the results of 1200 V and 1700 V IGBTs. The computer-aided TCAD simulations were performed using a simplified front-side IGBT structure to understand the uniform Al modification on all the measured DC-link voltages.

Keywords: IGBT, short-circuit, current filaments, aluminium modification.

INTRODUCTION

IGBTs are one of the frequently used power semiconductor devices in the field of power electronics. One of the important properties of the IGBT is SC robustness. Even though the IGBT has many advantageous features, it requires a detailed investigation regarding its physical limit during SC operation beyond the safe operating area (SOA).

The short-circuit safe operating area (SC-SOA) for different voltage classes ranging from 1200 V to 6500 V has been investigated in [1-6]. The results shown in [6], explain that IGBT SC destruction can be due to the formation of current filaments occurring at the collector side. These current destructions occur far beyond the SOA [7]. Further experimental investigations, carried out in [8], showed that it is possible to observe the current filaments in the IGBTs using Thermo-Reflectance Microscopy (TRM) under repetitive SC operation. A wide range of non-destructive current filaments was observed for IGBTs and these current filaments occur in a regular pattern [8]. The current filaments generate a similar pattern imprint visible as local Al modification under repetitive SC conditions. Hence, the optical microscope was used to study the local Al modification as an indicator of current filaments in 1200 V and 1700 V IGBTs [9-11]. Generally, for lower DC-link voltages, non-destructive current filaments can be observed under repetitive SC measurement. As the applied DC-link was increased, the filament pattern became finer, and transformed into a substantially homogeneous current distribution [11].

In the present work, repetitive SC measurements were performed on 50 A - 650 V class IGBTs with trench technology using an open, encapsulated chip soldered on a direct copper bonded (DCB) substrate. The repetitive SC measurements show a uniform Al modification of the emitter metallization irrespective of the DC-link voltages and collector current. Even though the SC pulse width was reduced, the Al modification remains uniform for all the measured SC conditions. These results were contrary to 1200 V and 1700 V IGBTs. Hence, TCAD simulations were carried out for 650 V IGBTs to study the reason for the homogenous Al modification at different DC-link voltages.

ALUMINIUM MODIFICATION THEORY

The study about Al surface modification on silicon due to thermal cycling was recorded in [12]. During power cycling, the change in the Al metallization was observed due to periodic stress [13]. This modification of the Al metallization due to compressive and tensile stress during heating and cooling phases leads to the protrusion or cavitation of single Al grains. Thereby, the roughness and electrical resistance of the Al metallization increases [13, 14, 15].

DOI: https://doi.org/10.14311/ISPS.2021.003

SETUP FOR REPETITIVE SHORT-CIRCUIT (SC) MEASUREMENT

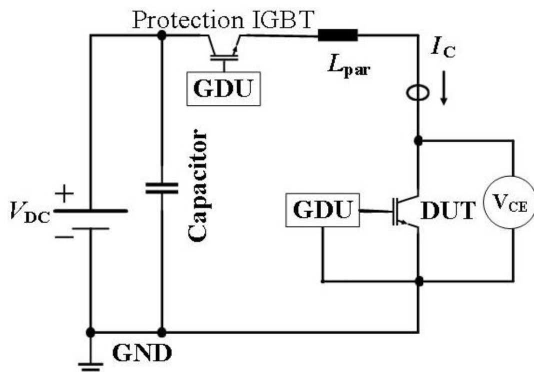

Fig. 1: Schematic of a SC type-1 measurement setup.

A schematic measurement setup used to measure the short-circuit of an IGBT is shown in Fig. 1. The protection IGBT and the device under test (DUT) were connected in series close to the DC-link capacitors to reduce the parasitic inductance of the SC path. A parasitic inductance L_{par} of the whole SC was 30 nH. The protection IGBT was used to limit the failure current in case of a DUT failure at the level of the SC current of the protection IGBT. Two gate drive units (GDU) were used to control the gate voltages V_{GE} of the DUT and the protection IGBT.

MEASUREMENT OF THE DESTRUCTIVE BOUNDARY LINE FOR 650 V IGBT

Before explicating the repetitive SC measurements, the destruction boundary limit of the 50 A - 650 V IGBTs was measured for two different temperatures (Fig. 2). For fixed V_{CE} = V_{DC}, the destruction current limit was measured by increasing the V_{GE} in steps of 0.25 V.
The critical collector current I_C as a function of V_{CE} of the last non-destructive SC type-1 pulse is plotted at

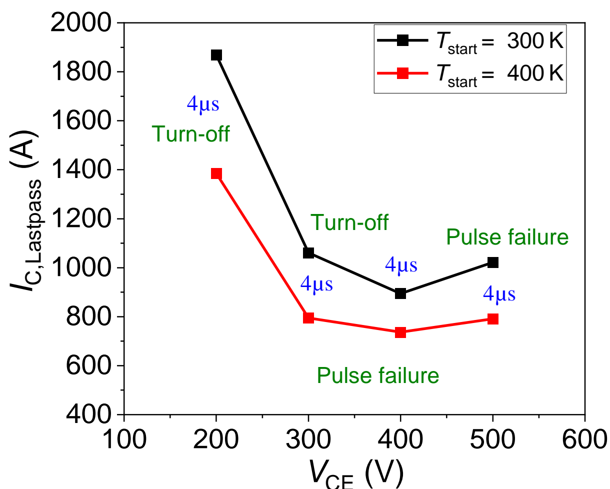

Fig. 2: Measured destruction limit of 650 V IGBTs far above the datasheet SC-SOA with measurement conditions L_{par} = 30 nH, $R_{G,ON}$ = 150 Ω, $R_{G,OFF}$ = 270 Ω.

300 K and 400 K in Fig. 2. An SC pulse width of 4 µs was set for all the last passed collector current measurements. For both temperatures, the minima of the destructive line occur at 400 V. In Fig. 2, the decrease in SC robustness far above the SC-SOA from 200 V to 400 V is due to the higher energy dissipation. Above 400 V, the SC capability increases due to the homogenous current distribution in the IGBT as the space-charge region covers the whole drift region with higher applied voltage and higher collector current [7]. For DC-link voltages of 200 V and 300 V, the destruction of the IGBT occurred during the SC turn-off, and for 400 V and 500 V during the SC pulse. A similar failure type occurs at higher temperatures. However, there is a significant reduction in the SC robustness of the IGBT device.

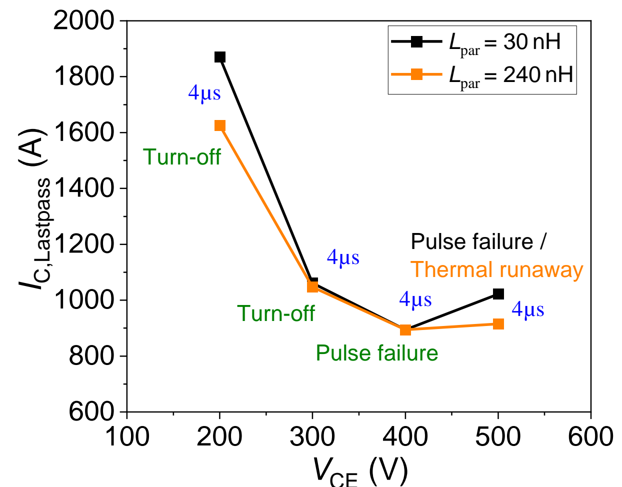

Fig. 3: Measured destruction limit of 650 V IGBTs for different parasitic inductances with measurement conditions $R_{G,ON}$ = 150 Ω, $R_{G,OFF}$ = 270 Ω, T_{start} = 300 K.

The parasitic inductance (L_{par}) is one of the important parameters under SC stress. The SC behavior of the IGBT can vary depending on $L_{par.}$ For two different parasitic inductances, the critical SC collector current of the IGBT is plotted in Fig. 3. For higher L_{par} measurements, the failure types are similar to lower parasitic inductance, except at 500 V. The reduced collector current at 200 V can be explained due to an increased SC turn-off voltage peak, which is shown and compared in Fig. 4(a) and (b). For a DC-link voltage 200 V and higher L_{par}, the maximum voltage during SC turn-off increases to 418 V compared to 234 V for lower L_{par}. Apparently, the turn-off peak voltage induced by the parasitic inductance L_{par} worsens the situation, so that the IGBT mostly fails during turn-off for lower DC-link voltages. For the non-destructive, last passed pulse, the critical energy will be higher for 240 nH in comparison to 30 nH. At higher L_{par}, the critical energy decreases with critical SC current showing that the turn-off overvoltage is an accelerating parameter [7]. Also, for higher parasitic inductance and at 500 V, the last passed collector current reduces due to a higher SC turn-off voltage peak. As this voltage peak is close to the rated

DOI: https://doi.org/10.14311/ISPS.2021.003

voltage of the device, thermal runaway of the device can occur.

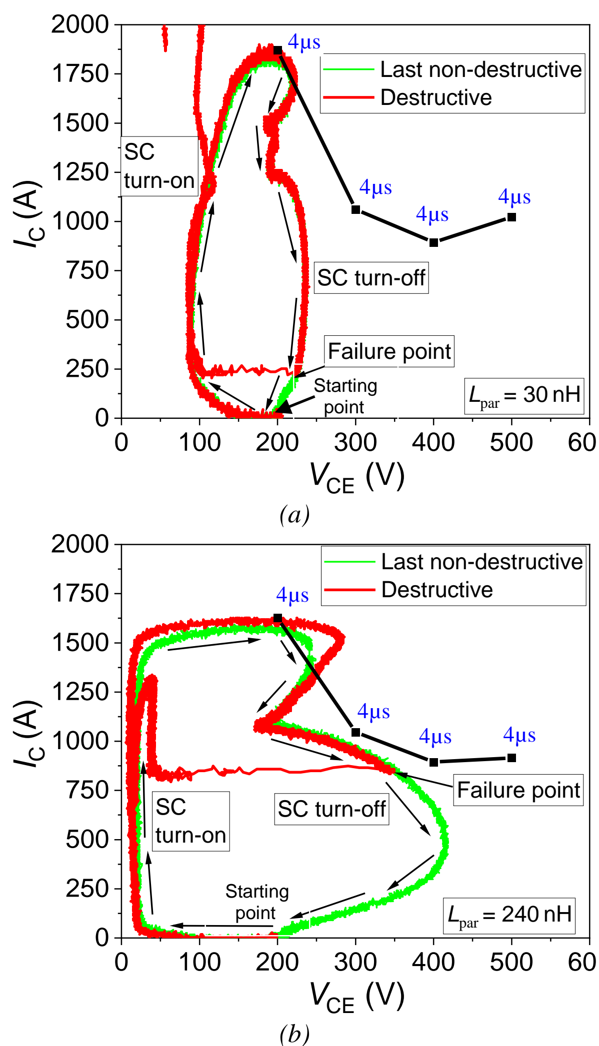

Fig. 4. SC in I_C-V_{CE} phase space diagram for last passed and destructive pulse at V_{DC} = 200 V, $R_{G,ON}$ = 150 Ω, $R_{G,OFF}$ = 270 Ω, T_{start} = 300 K. (a) L_{par} = 30 nH (b) L_{par} = 240 nH.

RESULTS OF REPETITIVE SHORT-CIRCUIT MEASUREMENTS

Fig. 5 displays an overview of the repetitive SC measurements carried out within the I_C-V_{CE} phase space. The black squares show the critical collector current as a function of V_{CE} of the last non-destructive SC pulse for the case that only single SC pulses were applied and the gate-emitter voltage was gradually increased until destruction occurred.

The scattered points in Fig. 5 indicate the operating conditions of the investigated IGBTs under repetitive SC events. The IGBT chips measured close to the destruction boundary line were able to survive few tens to hundreds of repetitive SC pulses. The devices which were destroyed during the repetitive SC pulses are marked with red squares along with the number of SC pulses survived. The blue stars represent the working samples after several hundreds or thousands of SC pulses away from the destructive boundary line.

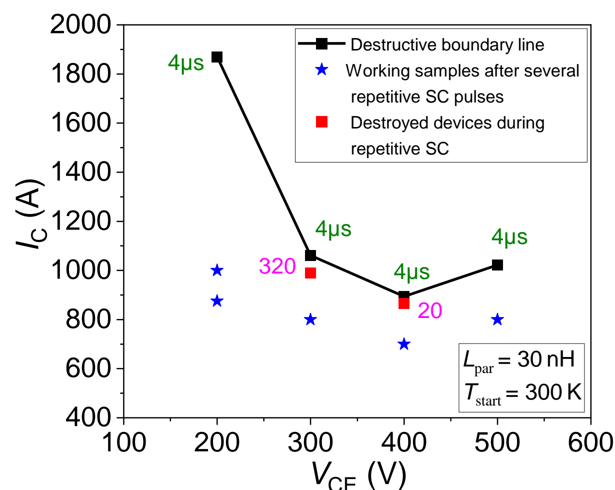

Fig. 5: Critical SC current of the last non-destructive pulse of a 650 V IGBT (black line), and test points for repetitive SC measurement in I_C-V_{CE} phase space (scattered points).

In order to observe the aluminium modification on the emitter metallization for defined conditions, the repetitive SC measurements were interrupted after a certain number of pulses. The optical microscope is used to observe the change in emitter-surface metallization. This technique can be used without additional effort on the measurement setup, and gives information about the Al modification. However, this method does not give any information about the temperature on the top-side metallization. This approach provides indirect information about the current distribution during SC. An initial picture of the top side of the unstressed IGBT was taken using an optical microscope before starting the repetitive SC events. For the defined measurement condition at a constant gate-emitter voltage (V_{GE}) and collector-emitter voltage (V_{CE}), the repetitive SC event was interrupted after a certain number of SC pulses, for example, 500 pulses, to take another picture of the top-side Al metallization. Afterwards, the next set of SC pulses was applied, and the measurements were repeated for several thousand SC pulses.

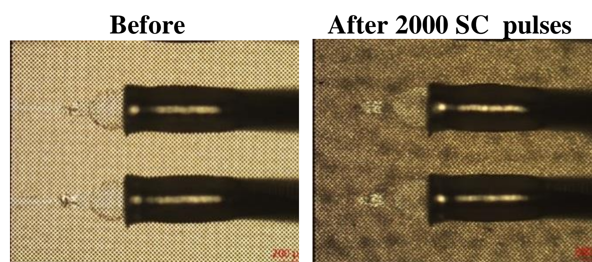

Fig. 6: Aluminium emitter surface analysis using optical microscope for a 1200 V IGBT at V_{DC} = 300 V, V_{GE} = 40 V, I_C = 300 A, t_{SC} = 4 µs, t_{gap} = 1 s, R_G = 220 Ω, $R_{G,OFF}$ = 270 Ω, and L_{par} = 45 nH [10].

The Al modification occurs during repetitive SC events due to a certain temperature swing [14]. When the device is subjected to the repetitive SC event, and if sufficient

DOI: https://doi.org/10.14311/ISPS.2021.003

temperature swing is generated due to the dissipated energy, the grain structures of the Al metallization modify. However, this process needs a certain amount of repetitive cycles as e.g. shown in Fig. 6. The 1200 V IGBT shows a clearly inhomogeneous aluminium modification as an indicator of current filaments as shown in Fig. 6 at DC-link voltage of 300 V [10].

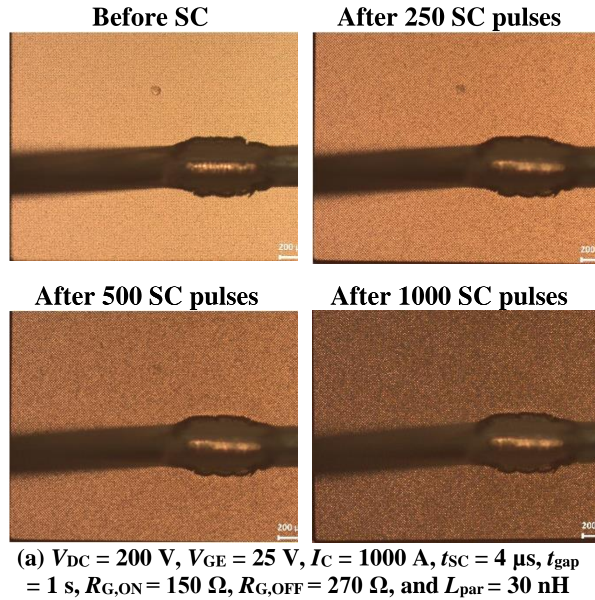

(a) V_{DC} = 200 V, V_{GE} = 25 V, I_C = 1000 A, t_{SC} = 4 µs, t_{gap} = 1 s, $R_{G,ON}$ = 150 Ω, $R_{G,OFF}$ = 270 Ω, and L_{par} = 30 nH

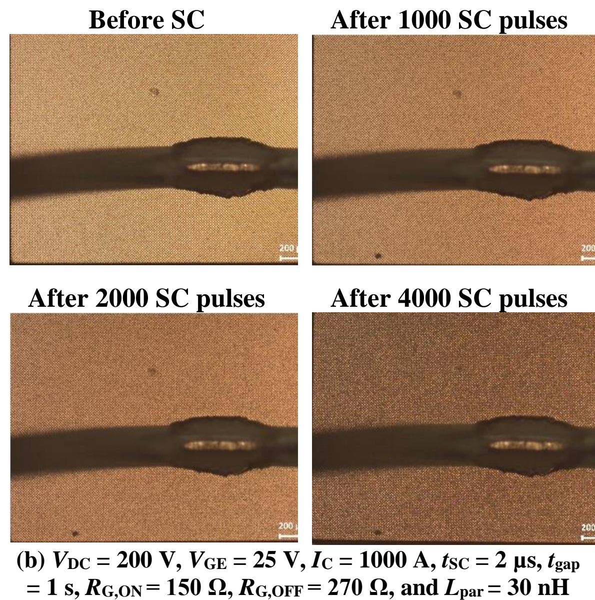

(b) V_{DC} = 200 V, V_{GE} = 25 V, I_C = 1000 A, t_{SC} = 2 µs, t_{gap} = 1 s, $R_{G,ON}$ = 150 Ω, $R_{G,OFF}$ = 270 Ω, and L_{par} = 30 nH

Fig. 7: Aluminium surface of a 650 V IGBT before and after series of SC pulses using optical microscope for different SC pulse width for given SC conditions (a) t_{SC} = 4 µs (b) t_{SC} = 2 µs.

The results in Fig. 7 show the Al modification compared for two different SC pulse widths for the same SC conditions. For t_{SC} = 4 µs, the 650 V IGBT shows a homogenous Al modification after 500 repetitive SC pulses. The change in temperature during the SC (ΔT_{SC}) will be higher for the 650 V IGBTs, compared to HV IGBTs, due to the smaller drift region [16]. Hence, the SC pulse width was halved to reduce the overall energy deposition during the SC and to make possible current filaments more visible in the metal imprint. Even though the SC pulse width was reduced to 2 µs during repetitive SC events in order to reduce the overall temperature influence on the emitter surface, no distinct metal-color change was visible. However, for t_{SC} = 2 µs, a higher number of repetitive SC events was required to modify the Al uniformly compared to the 4 µs pulse width. Furthermore, the collector current was reduced from 1000 A to 875 A for a SC pulse length of 4 µs in Fig. 8. The emitter metallization shows still a homogenous modification of Al after 1000 SC pulses.

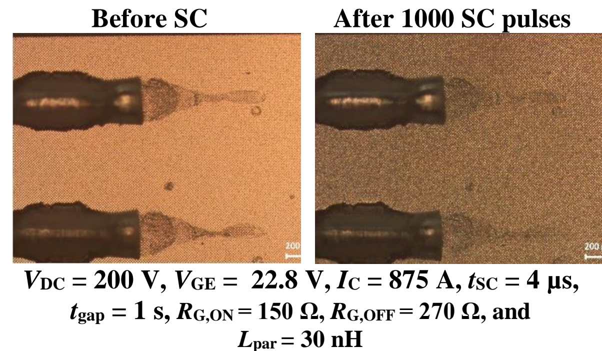

V_{DC} = 200 V, V_{GE} = 22.8 V, I_C = 875 A, t_{SC} = 4 µs, t_{gap} = 1 s, $R_{G,ON}$ = 150 Ω, $R_{G,OFF}$ = 270 Ω, and L_{par} = 30 nH

Fig. 8: Aluminium surface of a 650 V IGBT before and after series of SC pulses using an optical microscope with reduced collector current at V_{DC} = 200 V.

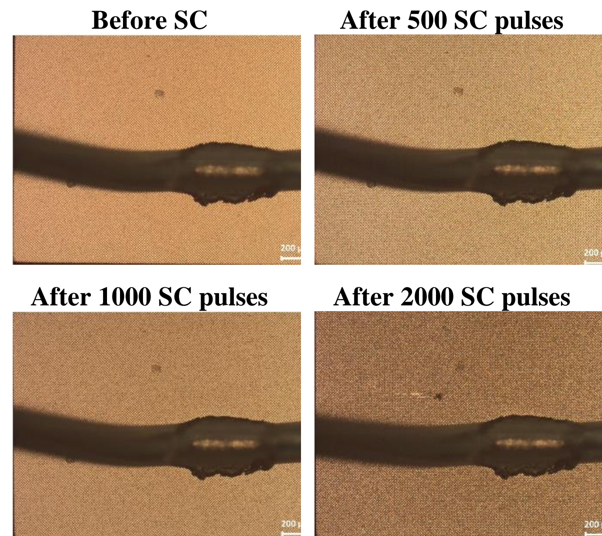

Fig. 9. Aluminium surface analysis of a 650 V IGBT using an optical microscope before and after series of SC pulses at V_{DC} = 300 V, V_{GE} = 20.8 V, I_C = 800 A, t_{SC} = 2 µs, t_{gap} = 1 s, $R_{G,ON}$ = 150 Ω, $R_{G,OFF}$ = 270 Ω, and L_{par} = 30 nH.

Fig. 9 exhibits the Al modification at 300 V and a collector current of 800 A. Here, a similar pattern to the repetitive measurements carried out at DC-link voltage of 200 V can be observed. The whole emitter metallization changes into a darker color with an increased number of SC pulses.

For both DC-link voltages at 200 V and 300 V, no clear local or inhomogeneous Al modifications for 650 V IGBTs were observable in contrast to the high-voltage class IGBTs (e.g., Fig. 6 in [9-11]). As 650 V IGBTs have a smaller base width, the high temperature from the back-side can reach the emitter

DOI: https://doi.org/10.14311/ISPS.2021.003

surface during a SC event with higher values. The temperature is more homogenous and higher throughout the emitter surface. These reasons can lead to a homogenous Al modification on the emitter side in 650 V IGBTs.

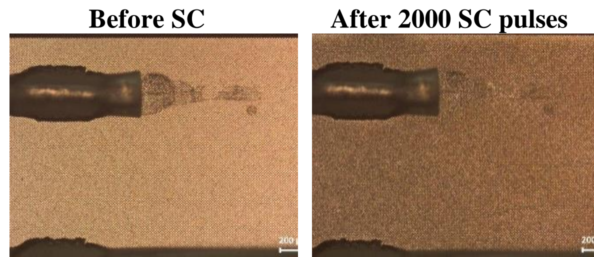

V_{DC} = 400 V, V_{GE} = 19.5 V, I_C = 700 A, t_{SC} = 2 µs, t_{gap} = 1 s, $R_{G,ON}$ = 150 Ω, $R_{G,OFF}$ = 270 Ω, L_{par} = 30 nH

Fig. 10: Aluminium surface of a 650 V IGBT chip at V_{DC} = 400 V and V_{GE} = 19.5 V.

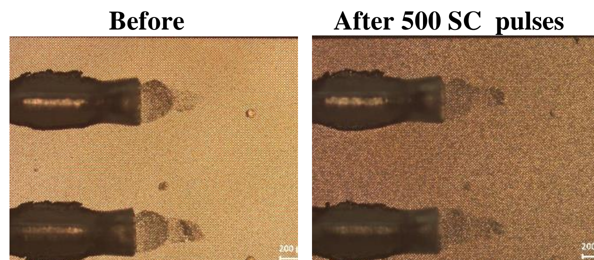

Fig. 11: Aluminium surface of a 650 V IGBT chip after a few hundred SC pulses at V_{DC} = 500 V and V_{GE} = 21 V.

Fig. 10 shows the Al modification development at V_{DC} = 400 V and V_{GE} = 19.5 V during 2000 SC pulses. The Al modification became stronger, and is distributed evenly after 2000 SC pulses. The SC duration was set to 2 µs for each pulse. Fig. 11 exhibits a similar Al modification after several hundred repetitive SC pulses at V_{DC} = 500 V and V_{GE} = 21 V. In both cases, a uniform Al surface modification appeared. The homogenous Al modification at 400 V and 500 V is in accordance with high-voltage class IGBTs under repetitive SC measurements [9-11].

ELECTRO-THERMAL SHORT-CIRCUIT SIMULATION RESULTS

In this section, electro-thermal SC simulations are shown for 650 V and 1200 V IGBTs using Sentaurus TCAD. This simulation result helps to understand the reason for homogenous Al modification irrespective of DC-link voltages for 650 V IGBTs. The device simulation was carried out to study the current filament formation and to estimate the surface temperature during a SC pulse with current filaments in the chip. A simplified front-side IGBT structure was used to investigate the current filament behavior under different V_{DC} and I_C conditions [6]. This IGBT structure is 200 µm wide. A simple time-dependent SC current pulse was simulated with a 300 K starting temperature (T_{start}), L_{par} =30 nH and with a constant DC-link voltage. For the SC simulation, the Phillip's unified mobility model, University of Bologna avalanche model, Shockley-Read-Hall (SRH) and Auger recombination models and Slotboom model for effective intrinsic density were utilized. For the SC simulation, self-heating was considered with a thermal boundary condition at the drain contact and a thermal resistance of 3.22 K/W. For simulation at 1200 V IGBT structure in [9], the SC pulse width was set to 4 µs, which was also used for this paper. However, the pulse width was reduced to 2.5 µs for 650 V IGBT during SC simulation in order to reduce the deposited energy during the SC.

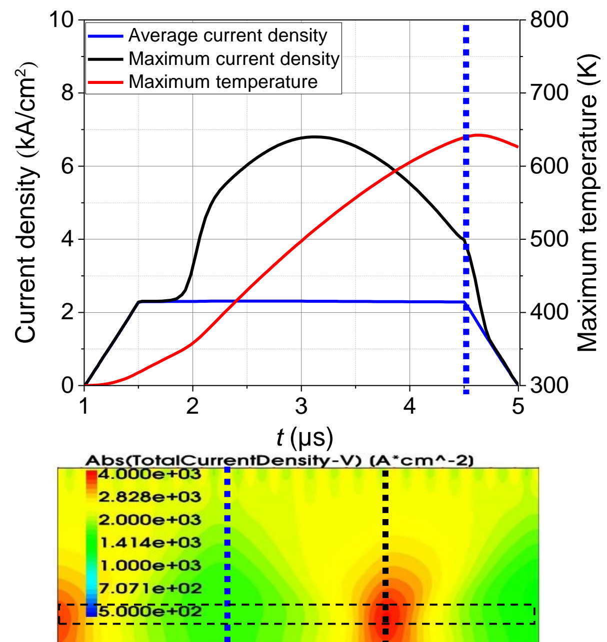

Fig. 12: (Top) Transients of the maximum and the average current density and the transient of the maximum temperature from electro-thermal short-circuit simulation at V_{DC} = 400 V, I_C = 235 A, T_{start} = 300 K (Bottom) current density distribution at 4.5 µs for 1200 V IGBT.

For 1200 V IGBTs, a clear local Al modification under repetitive SC stress using microscopy has been observed as shown in Fig. 6, and explained through simulation in [9,10]. The SC simulation was performed for 1200 V IGBT class at V_{DC} = 400 V, I_C = 235 A, T_{start} = 300 K and SC pulse length (t_{SC}) of 4 µs. In Fig. 12, the top picture shows the transients of the average and maximum current densities and the transient of the maximum temperature during the SC event for the above mentioned SC condition. The rise time and fall time was set to 0.5 µs. The bottom picture in Fig. 12 shows the absolute total current density in the IGBT at 4.5 µs. The average and maximum current densities were extracted from a window near the *n*-base/*n*-field-stop junction. The maximum temperature was extracted from the whole silicon region. At 1.8 µs, the average and maximum current densities start to split. The current flow becomes inhomogeneous. The slope of the maximum temperature transient increases slightly after 2 µs. For the simulated structure of 200 µm, there are one and a half current filaments at 4.5 µs during SC as shown in bottom Fig. 12. The edge-to-edge lateral distance between the current filaments is 110 µm.

DOI: https://doi.org/10.14311/ISPS.2021.003

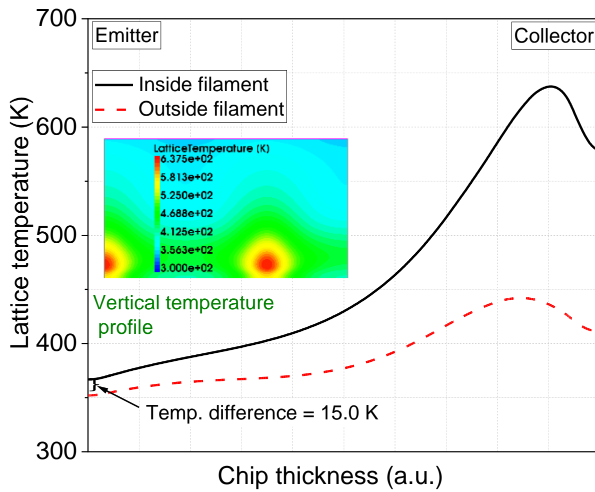

Fig. 13: Lattice temperature distribution in a 1200 V IGBT during SC simulation at V_{DC} = 400 V, I_C = 235 A, T_{start} = 300 K at 4.5 µs, for cuts ref. to Fig. 12 (bottom). Inset: IGBT lattice temperature distribution at 4.5µs.

The lattice temperature distribution of the 1200 V IGBT during SC simulation at 4.5 µs is shown in Fig. 13. The positions of the vertical cross sections are inside and outside the current filament and marked in Fig. 12 (bottom). The temperature reaches a maximum value of 630 K inside the current filament, and a value of 490 K outside the current filament at the collector side. The temperature at the emitter-side reduces as the temperature propagates from back-side to front-side. The temperature at the emitter surface above the filament area shows a value of 366 K, which is 15 K higher than the emitter surface above the non-filament area as shown in Fig. 13.

The short-circuit simulations were carried out for 650 V IGBTs with t_{SC} of 2.5 µs. In Fig. 14 (top) the picture shows the transients of the average current density, maximum current density and maximum temperature during the SC event at V_{DC} = 200 V, I_C = 1500 A, and T_{start} = 300 K. The average and maximum current densities were extracted from the window shown in the current density distribution bottom picture in Fig. 14. As soon as the average and the maximum current density start to split at 2.75 µs, the current flow becomes inhomogeneous. The current distribution at time point 3.1 µs is depicted in the bottom picture in Fig. 14. There are four and a half current filaments for the 200 µm simulated structure. These filaments have an edge-to-edge lateral distance of 30 µm ± 6 µm. Hence, there are more current filaments for 650 V IGBTs in comparison to 1200 V IGBT (see Fig. 12) for the given area. Furthermore, the increase in simulated SC pulse width leads to higher homogenous distribution at the emitter side.

Fig. 15 shows a vertical cross section of the absolute value of the electric-field strength, electron density and hole density in the IGBT structure at time point 3.1 µs.

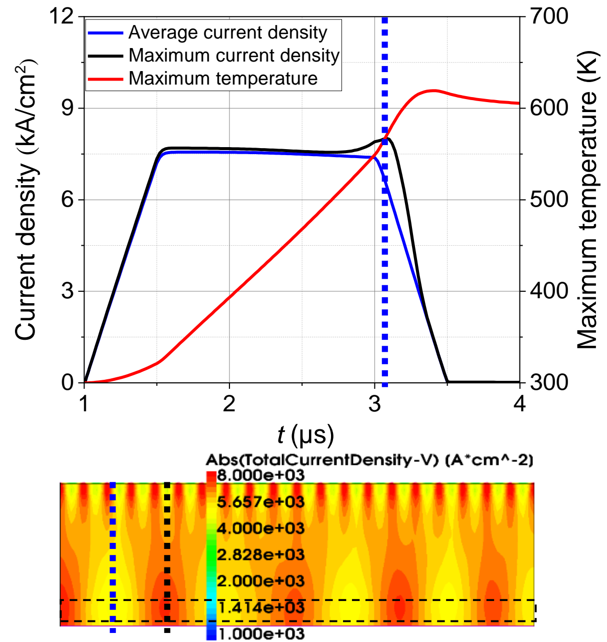

Fig. 14: (Top) Transients of the maximum and the average current density and the transient of the maximum temperature from electro-thermal short-circuit simulation at V_{DC} = 200 V, I_C = 1500 A and T_{start} = 300 K (Bottom) current density distribution at 3.10 µs for 650 V IGBT.

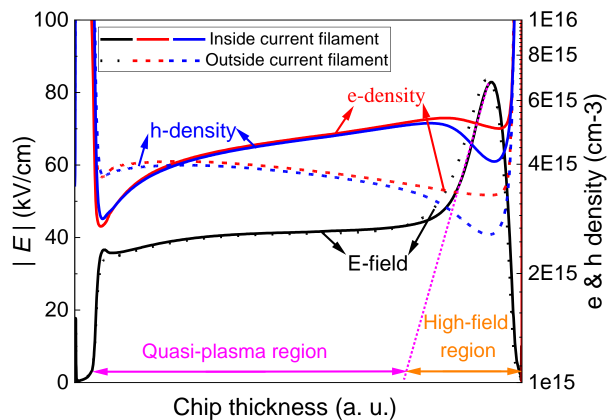

Fig. 15: Absolute value of the electric-field strength, electron and hole density distribution in IGBTs during SC simulation at V_{DC} = 200 V, I_C = 1500 A, T_{start} = 300 K at 3.1 µs, vertical cuts marked in Fig. 14 (bottom).

The positions of the vertical cross sections are marked inside and outside the current filament in Fig. 14 (bottom). For 650 V IGBTs, the electric field strength remains approximately the same inside and outside the current filament. However, the electron and hole density varies in the filament and non-filament area. As the current constricts in the current filament, the electron and hole densities are two times higher in comparison to the outside filament cut. From the simulation, there is a correlation between the lateral distance between the filaments and the width of the quasi-plasma region. The width of the high-field region defines the diameter of the current filament [11], see Fig. 14 (bottom). For 650 V IGBTs, the drift region is smaller, hence a smaller high-field region leads to a higher number of current filaments.

DOI: https://doi.org/10.14311/ISPS.2021.003

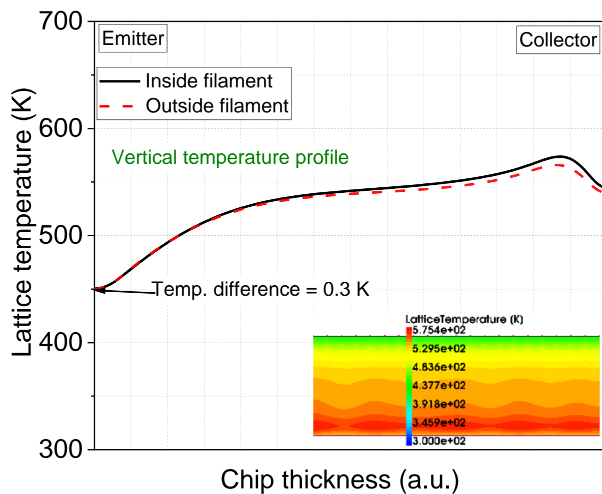

Fig. 16: Lattice temperature distribution in a 650 V IGBT during SC simulation at V_{DC} = 200 V, I_C = 1500 A, T_{start} = 300 K at 3.1 µs, for cuts ref. to Fig. 14 (bottom). Inset: IGBT lattice temperature distribution at 3.1 µs.

For 650 V IGBT, the lattice temperature distribution inside and outside the filament area is plotted in Fig. 16 at 3.1 µs during the given SC conditions. At the collector side, the temperature difference between inside and outside filament is 10 K. The temperature at the emitter surface above the filament area is 450 K. The emitter surface temperature above the non-filament area is similar to the temperature found in the emitter region above the filament area. The temperature difference between these two emitter areas is 0.3 K. For 650 V IGBTs, the emitter surface temperature is very high and the difference in the emitter surface temperature between inside and outside filament position is approximately the same. This may be the reason for homogenous Al modification at 200 V DC-link.

In Fig. 17 (top) the picture shows the transients of the average current density, maximum current density and maximum temperature at V_{DC} = 300 V, I_C = 855 A during SC. Under these conditions, even weaker filaments are seen with slightly increased lateral spacing between two neighbouring filaments as shown in Fig. 17 (bottom). The average and maximum current densities were extracted from the window shown in the current density distribution bottom picture in Fig. 17. The maximum temperature during the SC is 565 K at 3.4 µs. For DC-link voltage of 300 V, the number of filaments has reduced to four in comparison to 200 V. The edge-to-edge lateral distance between current filaments is 35 µm ± 5 µm.

The vertical cross section of the absolute value of the electric-field strength, electron density and hole density in the IGBT structure at time point 3.0 µs for given SC conditions is shown in Fig. 18. The positions of the vertical cross sections are marked inside and outside the current filament in Fig. 17 (bottom). The electric field strength remains approximately the same inside and outside the current filament as shown in Fig. 18. The electron and hole density varies in the filament and non-filament areas.

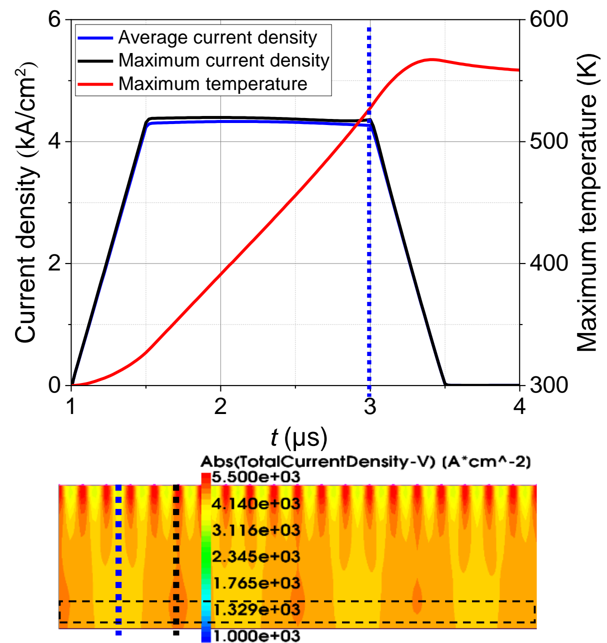

Fig. 17: (Top) Transients of the maximum and the average current density and the transient of the maximum temperature from electro-thermal short-circuit simulation at V_{DC} = 300 V, I_C = 855 A and T_{start} = 300 K (Bottom) current density distribution at 3.00 µs for a 650 V IGBT.

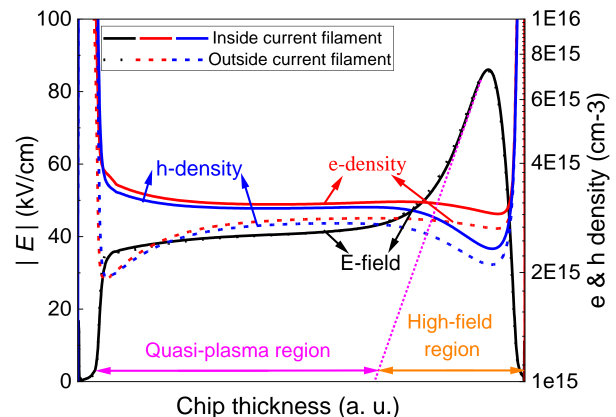

Fig. 18: Absolute value of the electric-field strength, electron and hole density distribution in a 650 V IGBT during SC simulation at V_{DC} = 300 V, I_C = 855 A, T_{start} = 300 K at 3.0 µs, vertical cuts marked in Fig. 17 (Bottom).

The temperature distribution inside and outside the filament region is approximately the same as shown in Fig. 19 for 650 V IGBT at 300 V DC-link voltage. A slightly lower temperature of 434 K is seen on the emitter surface in comparison to 200 V SC conditions.

The current distribution became homogeneous above 400 V. The SC simulation results at 500 V is exemplified in Fig. 20. The split in average and maximum current density was very small. The current flow is uniform throughout the device.

DOI: https://doi.org/10.14311/ISPS.2021.003

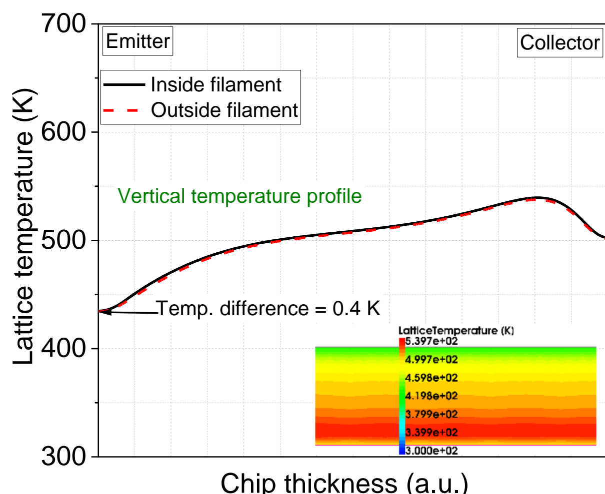

Fig. 19: Lattice temperature distribution in a 650 V IGBT during SC simulation at $V_{DC} = 300$ V, $I_C = 855$ A, $T_{start} = 300$ K at 3.0 µs, for cuts ref. to Fig. 17 (bottom). Inset: IGBT lattice temperature distribution at 3.0µs.

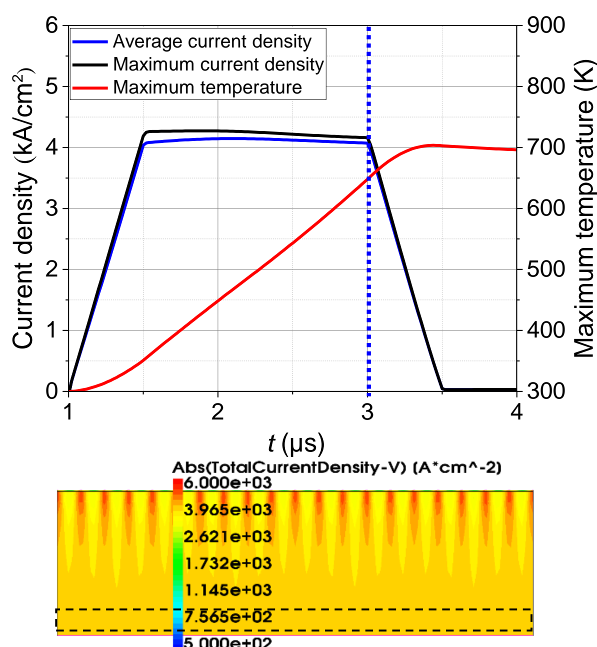

Fig. 20: (Top) Transients of the maximum and the average current density and the transient of the maximum temperature from electro-thermal short-circuit simulation at $V_{DC} = 500$ V, $I_C = 820$ A and $T_{start} = 300$ K (Bottom) current density distribution at 3.00 µs for a 650 V IGBT.

CONCLUSION

In 650 V IGBT short-circuit measurements, the dependence of the critical collector current as a function of DC-link voltage is similar to that of the high voltage IGBT class. As the DC-link voltage increases, the collector current decreases and increases after reaching a minimum. In repetitive SC measurements, homogenous Al modifications were observed at 200 V and 300 V DC-link voltage. Generally, the appearance of current filaments is expected at these DC-link voltages, which is supported by the performed electro-thermal SC simulations. Furthermore, the 650 V IGBT shows a higher amount of these current filaments during SC for the simulated structure width of 200 µm in comparison to the 1200 V IGBT structure due to the smaller quasi-plasma region. Even though the SC pulse width was reduced to 2.5 µs during the SC event, the 650 V IGBTs show a much higher emitter surface temperature in comparison to the 1200 V simulated IGBT due to the smaller base width. However, whereas the temperature difference at the emitter surface between the filament and non-filament region is 15 K for 1200 V IGBT, it is significantly smaller for a 650 V IGBT structure. This explains why the homogenous Al modification on the emitter metallization of 650 V IGBTs occurs although current filaments are present at the collector side.

ACKNOWLEDGEMENTS

The authors would like to thank Abhishek Maitra for his help during the repetitive short-circuit measurements.

REFERENCES

[1] A. Kopta, M. Rahimo, U. Schlapbach, at el, "Limitation of the Short-Circuit Ruggedness of High Voltage IGBTs," in Proc. ISPSD, 2008, pp. 33-36.

[2] R. Baburske, V. Treek, F. Pfirsch, F. J. Niedernostheide, at el, "Comparison of Critical Current Filaments in IGBT Short Circuit and during Diode Turn-off," in Proc. ISPSD, 2014, pp. 47-50.

[3] H. Hagino, J. Yamashita, A. Uenishi, at el., "Avalanche Characteristics and Failure Mechanism of High Voltage Diodes," IEEE Transactions on Electron Devices, Vol. ED-13, No. 11, pp. 754-758, 1996.

[4] M. Tanaka, A. Nakagawa, "Simulation studies for Avalanche induced short-circuit current crowding of MOSFET-Mode IGBT," in Proc. ISPSD, 2015, pp. 121-124.

[5] M. Tanaka, A. Nakagawa, "Growth of short-circuit current filament in MOSFET-Mode IGBTs," in Proc. ISPSD, 2016, pp. 319-322.

[6] R. Bhojani, S. Palanisamy, R. Baburske, et al, "Simulation study on collector side filament formation at short-circuit in IGBTs," in Proc. of ISPS, Prague, Czech Republic, 2016, pp. 70-76.

[7] R. Baburske, F. J. Niedernostheide, H.-J. Schulze, at el, "Unified view on energy and electrical failure of the short-circuit operation of IGBTs," Microelectronics Reliability, 2018, Vol. 88-90, pp. 236-241.

[8] R. Bhojani, J. Kowalsky, J. Lutz, D. Kendig, R. Baburske, H. J. Schulze, F. J. Niedernostheide, "Observation of Current Filaments in IGBTs with Thermo-Reflectance Microscopy," in Proc. ISPSD, May 2018, pp. 164-167.

DOI: https://doi.org/10.14311/ISPS.2021.003

[9] R. Bhojani, J. Kowalsky, J. Lutz, at el, “Local Aluminium Modification as Indicator for Current Filaments in IGBTs far beyond the Safe Operating Area,” in Proc. of ISPS, Prague, Czech Republic, August 2018, pp. 97-104.

[10] M-L. Mysore, R. Bhojani, J. Kowalsky, at el., “Al Modification as Indicator of Current Filaments in IGBTs under repetitive SC operation,” Transactions on IET power electronics, ISSN 1755-4535, pp. 1-10, 2019.

[11] R. Bhojani, M-L. Mysore, R. Raihan at el, “Current Filament Behavior in Different Voltage Class IGBTs using Measurements and Simulations,” in Proc. ISPSD, Sep. 2020, pp. 446-449.

[12] C. J. Santoro: “Thermal Cycling and Surface Reconstruction in Aluminium Thin Films,” J. Electrochem. Soc., Vol. 116, 1969, pp. 361-364.

[13] M. Ciappa, P. Malberti, “Plastic-Strain of Aluminium Interconnections during Pulsed Operation of IGBT Multichip Modules,” Qual. and Reliab. Eng. Int. 12, 1996, pp. 297-303.

[14] J. Lutz, H. Schlangenotto, et al, Semiconductor Power Devices-Physics, Characteristic, Reliability. Springer, Second edition, 2018.

[15] M. Ciappa: “Selected failure mechanisms of modern power modules,” Microelectronics Reliability, Vol. 42, 2002, pp. 653-667.

[16] T. Basler, R. Bhojani, J. Lutz, at el, “Measurement of a complete HV IGBT I-V characteristic up to the breakdown point,” EPE, 2013, ECCE Europe, Lille, France.

Addresses of the authors

Madhu-Lakshman Mysore, Reichenhainer Str. 70, Chemnitz, Germany, madhu-lakshman.mysore@etit.tu-chemnitz.de
Thomas Basler, Reichenhainer Str. 70, Chemnitz, Germany, thomas.basler@etit.tu-chemnitz.de
Josef Lutz, Reichenhainer Str. 70, Chemnitz, Germany, josef.lutz@etit.tu-chemnitz.de
Roman Baburske, Infineon Technologies AG, Neubiberg, Germany, roman.baburske@infineon.com
Hans-Joachim Schulze, Infineon Technologies AG, Neubiberg, Germany, schulze.external9@infineon.com
Franz-Josef Niedernostheide, Infineon Technologies AG, Neubiberg, Germany, franz-josef.niedernostheide@infineon.com